



Institut für Numerische Simulation
Rheinische Friedrich-Wilhelms-Universität Bonn

Wegelerstraße 6 • 53115 Bonn • Germany
phone +49 228 73-3427 • fax +49 228 73-7527
www.ins.uni-bonn.de

J. S. Dolado, M. Griebel, and J. Hamaekers

**A Molecular Dynamics Study of Cementitious
Calcium Silicate Hydrate (C-S-H) Gels**

INS Preprint No. 0701

May 2007

A Molecular Dynamics Study of Cementitious Calcium Silicate Hydrate (C-S-H) Gels*

J. S. Dolado

LABEIN-Tecnalia, Parque Tecnológico de Bizkaia, Derio, Spain.

*Nanostructured and Eco-efficient Materials for Construction Unit, Associated Unit
LABEIN-Tecnalia/CSIC, Derio, Spain.*

M. Griebel and J. Hamaekers

Institute for Numerical Simulation, University of Bonn, Germany.

Abstract

In this article we study the polymerization of silicic acids ($\text{Si}(\text{OH})_4$) in the presence of calcium ions by molecular dynamics simulations. We focus on the formation and structure of cementitious calcium silicate hydrate (C-S-H) gels. Our simulations confirm that, in accordance with experiments, a larger content of calcium ions slows down the polymerization of the cementitious silicate chains and prevents them from forming rings and three-dimensional structures. Furthermore, by an analysis of the connectivity of our simulated silicate chains and by a count of the number of formed Ca-OH and Si-OH bonds, the relationship with commonly employed structural models of calcium silicate hydrate (C-S-H) gels, such as 1.4-nm tobermorite and jennite, is discussed.

1 Introduction

Calcium silicate hydrate (C-S-H) gel is definitely the most important hydration product of cement based materials. It constitutes about 60-70 % of the fully hydrated cement paste and is responsible for most of the properties of cement-based

*This work has been supported by the Basque Government (NANOMATERIALES and HIBRICEM projects), the Spanish Government (project MONACEM (Ref-MAT2005-03890)), and, in parts, by the Schwerpunktprogramm 1165 and the Sonderforschungsbereich 611 of the Deutsche Forschungsgemeinschaft.

materials. From a compositional point of view, C-S-H gel is often characterized by its Ca/Si ratio, which typically ranges from 0.7 to 2.3. This variability in composition explains why, though intensively studied by techniques like SEM, TEM, NMR, etc [1], many features of the nanostructure of C-S-H gel remain unknown.

Much of the existing knowledge on the nanostructure of C-S-H gel has been gained from structural comparisons with crystalline calcium silicate hydrates. In fact, several models [2–7] have been proposed so far that draw structural analogies with tobermorite and jennite crystals and/or with distorted semi-crystalline variations of them (the so called C-S-H (I) and C-S-H (II) phases respectively). From these models, C-S-H gels can be approximately viewed as layered structures, in which calcium oxide sheets are ribbed on either side with silicate chains, and free calcium ions and water molecules are present in the interlayer space.

However, it is well experimentally established [1, 4, 8] that, if the structure of the C-S-H gel is actually composed of tobermorite and jennite pieces, these components should show multiple defects and imperfections. In fact, in view of their ^{29}Si NMR experiments, Cong and Kirkpatrick [4] proposed a structural model which is based on depolymerized and distorted tobermorite-like structures. According to this model, the Ca/Si ratio for perfect 1.4-nm tobermorite crystals (Ca/Si=0.8) could be raised to the values found in cementitious C-S-H gels (which typically is 1.7 on average) by the omission of bridging tetrahedrons, by the omission of entire segments of silicate chains or by the inclusion of tiny $\text{Ca}(\text{OH})_2$ environments. Similar conclusions were drawn from posterior ^{17}O NMR [9] and infrared (IR) measurements [10]. However, and contrary to this model which stresses the importance of tobermorite-like structures, different experiments have highlighted the importance of jennite crystals in appropriate structural models for cementitious C-S-H gels. Viehland et al. [11] and Zhang et al. [12] concluded from high resolution TEM observations that cementitious C-S-H gels contain both tobermorite-like and jennite-like spacings. Similarly, Thomas et al. [13] have recently employed inelastic neutron spectroscopy (INS) as quantitative probe of the content of Ca-OH bonds in decalcified cementitious pastes. They found relatively large concentration of Ca-OH bonds, a fact which confirms the presence of jennite-like features within the C-S-H gels.

In this situation, where the debate about the short-range ordering of cementitious C-S-H gel is still unsettled, any hint on the structure of C-S-H gels which can be provided by modeling and numerical simulation techniques would be tremendously beneficial. Some attempts have been already made in this direction. So far, most of these studies [14] have paid attention to the analysis of the cohesion of the C-S-H layers. To this end, structureless charged platelets of C-S-H embedded in a counterion-rich electrolyte solution were employed, where the interlayer forces were simulated either within the framework of the Deryaguin-Landau-Verwey-Overbeek (DLVO) theory [15, 16] or by Monte Carlo simulations [17, 18]. Furthermore there are a few attempts that account for atomistic level descriptions of the C-S-H gel [19–21]. All of these studies assume crystalline

tobermorite structures only. There is also a new approach followed recently by Manzano et al. [22], where the formation of C-S-H structures was analyzed by means of ab-initio calculations without imposing any structural model. Interestingly, two different growth mechanisms were identified that depend on the amount of Si and Ca ions which naturally lead to the appearance of both tobermorite-like and jennite-like nano-crystals.

In this article we study the formation and the structure of small cementitious C-S-H particles by the method of molecular dynamics. To this end, we numerically reproduce the formation of C-S-H structures and analyze the polymerization of silicic acids ($\text{Si}(\text{OH})_4$) in a calcium rich environment. In particular, our objective is twofold: On the one hand we provide information about interesting statistical quantities based on the connectivity of the silicate chains. On the other hand, we analyze the formation of Si-OH and Ca-OH bonds. In both cases special effort is put into the consequences on the structural models of C-S-H gels. Thus, our results provide new important insight into the C-S-H structure and its formation and may serve as starting point for future studies.

The remainder of this paper is organized as follows. Section 2 describes computational details and applied approximations. Section 3 presents the obtained results. Section 4 summarizes main findings and conclusions of the work.

2 Computational Procedure

The polymerization of silica sols ($\text{Si}(\text{OH})_4$ monomers) was first simulated with help of the molecular dynamics method by Feuston and Garofallini [23]. This pioneering work introduced an efficient potential function that describes the most basic and significant features of systems which contain Si, O and H interactions. The resulting model accounts especially well for forward condensation reactions. Here, the corresponding overall potential energy function is composed of a modified Born-Mayer-Huggins (BMH) two-body interaction term and a three-body interaction term similar to the well-known Stillinger-Weber [24] potential.

In this article, we apply such a molecular dynamic approach to study the formation of C-S-H structures that stem from the polymerization of silica sols in a calcium rich environment. To this end, we apply the type of potential energy function mentioned above to model Si, O and H interactions, but we use the improved variant of Litton and Garofalini. The detailed potential functions and parameters can be found in the literature [25]. To model the Si, O and Ca interactions we employ the variant given by Su and Garofalini [26]. Additionally, we apply a screened Coulomb potential term $\frac{q_i q_j}{r_{ij}} \text{erfc}(r_{ij}/\beta_{ij})$ to represent the repulsive interaction of Ca and H. Here, q_i denotes the ionic charge of particle i , r_{ij} denotes the distance between particle i and particle j , β_{ij} is an interaction-dependent parameter, and erfc stands for the complementary error function. For the parameter β_{ij} we use a value of 2.31 Å for an atom pair Ca-H. The ionic

charges for calcium ions and hydrogen are +2 and +1, respectively.

We use a so-called Nosé Langrangian [27] and employ periodic boundary conditions to perform molecular dynamics simulations in the canonical ensemble (NVT). To solve the corresponding equations of motion we apply a predictor-corrector scheme based on Beeman's approach [28] with the modifications due to Refson [29]. In the simulations, we use a time step size of 0.1 fs for the time integration scheme and set the fictitious mass parameter of the Nosé thermostat to a value of 100 u\AA^2 . The unit cell dimensions of all simulated periodic systems are $44 \text{ \AA} \times 44 \text{ \AA} \times 44 \text{ \AA}$. Thus we can employ the well-known linked cell technique together with a straightforward domain decomposition approach for an efficient parallel implementation. The potential terms were here cut off at a radius of 5 \AA . We incorporated the above-mentioned potential model into our existing molecular dynamics software package TREMOLO which is a load-balanced distributed memory parallel code [30]. This allows to simulate systems with large numbers of particles over long times in a reasonable computational time. All simulations were performed on the Himalaya cluster [31] at the Institute for Numerical Simulation at the University of Bonn. For further algorithmic and implemental aspects see Ref. [32].

In our numerical experiments four Ca/Si ratios were studied, namely Ca/Si=0.7, Ca/Si=1, Ca/Si=1.4 and Ca/Si=2. The number of atoms per cell and the densities of the studied systems are presented in Table 1. To simulate these four systems, we randomly placed appropriate amounts of Si(OH)_4 and $\text{Ca(OH)}_2 \cdot 4\text{H}_2\text{O}$ molecules into a cubic simulation cell.

Table 1: Number of atoms and densities

Ca/Si	Number of atoms	Density [g/cm ³]
0.7	6304	1.36
1.0	6728	1.47
1.4	7080	1.58
2.0	7448	1.71

To eliminate the effect of the initial atomic configuration, we first employed an NVT ensemble at 300 K over 10 ps. Then, for the next 90 ps, we linearly increased the temperature to a value of 1800 K. This high temperature was used to accelerate polymerization and to reduce drastically the computational time, following the approach by Garofalini and Martin [33] and Feuston and Garofallini [23]. Then, the NVT ensemble was performed over 1500 ps at 1800 K. Next we linearly decreased the target temperature over 500 ps to a value of 300 K. Finally, the NVT ensemble was applied over 100 ps at 300 K. Here, we counted the number and type of siloxane bonds (Si-O-Si) and the number of Si-OH and Ca-OH bonds. The distances we use to characterize bonds are given in Table 2. Note that all computed values have been averaged over the last 50 ps at 300 K of the simulation.

Table 2: Bond types and distances

Bond type	Distance [Å]
Si-O	2.3
Ca-O	2.6
O-H	1.3

3 Results and Discussion

3.1 Connectivity of the Silicate Chains

Nuclear magnetic resonance (NMR) techniques have proved to be suitable tools to follow the polymerization of the silicate species [1, 4, 8, 34]. There, a Q_n nomenclature is used in general for the peaks. Q_n is the chemical shift of a silicon atom which is bound to n bridging oxygens.

The time evolution of our calculated Q_n distributions are represented in Figure 1 for the following Ca/Si ratios: Ca/Si=0.7 (a), Ca/Si=1 (b), Ca/Si=1.7 (c), and Ca/Si=2 (d). The consumption of monomers ($\text{Si}(\text{OH})_4$) to yield longer silicate chains by condensation reactions ($\text{Si-OH} + \text{OH-Si} \leftrightarrow \text{Si-O-Si} + \text{H}_2\text{O}$) is usually assessed by the so called polymerization degree P (%). This parameter is written in terms of the Q₀ (%) as $P (\%) = 100 - Q_0 (\%)$. Thus, high values of Q₀ mean slow polymerizations and vice versa.

As shown in Figure 1, the number of Q₀ species decreases more slowly when the Ca/Si ratio is increased. In fact, after 2000 ps of simulation time, the polymerization degree P (or similarly Q₀) ranges from values of about 70 % (30 %) for Ca/Si=0.7 to values of about 30 % (70 %) for Ca/Si=2. This shows that the presence of Ca ions slows down the polymerization process of the silicate chains.

The Q₃ and Q₄ peaks deserve further discussion. The existence of such peaks is related to the appearance of three-dimensional structures (branched silicates in the case of Q₃ and rings in the case of Q₄ peaks). In Figure 2 (a) the sum of Q₃ and Q₄ peaks is represented as a function of the Ca/Si ratio (solid points). To better see the trend, also the best linear fit is shown (solid line). The experimental value found in Ref. [4] for Ca/Si=0.79 is represented by a square. It can be seen that the sum Q₃+Q₄ decreases linearly when the Ca/Si ratio is raised. Note that for Ca/Si=0.7, the percentage of three-dimensional morphologies still represents the 15 % of the Q_n distributions, whereas for Ca/Si=2 the non-linear forms have disappeared. Thus, these results indicate that the presence of calcium ions enforces the formation of linear structures in the polymerization process of silicic acids. This is in accordance with the experimental evidence in cementitious and synthetic C-S-H systems, where linear structures are completely dominant [1, 4]. Note that the non-vanishing values found for the Q₃+Q₄ (%) at low Ca/Si ratios can be seen as an indication of the presence of cross-linkages between the

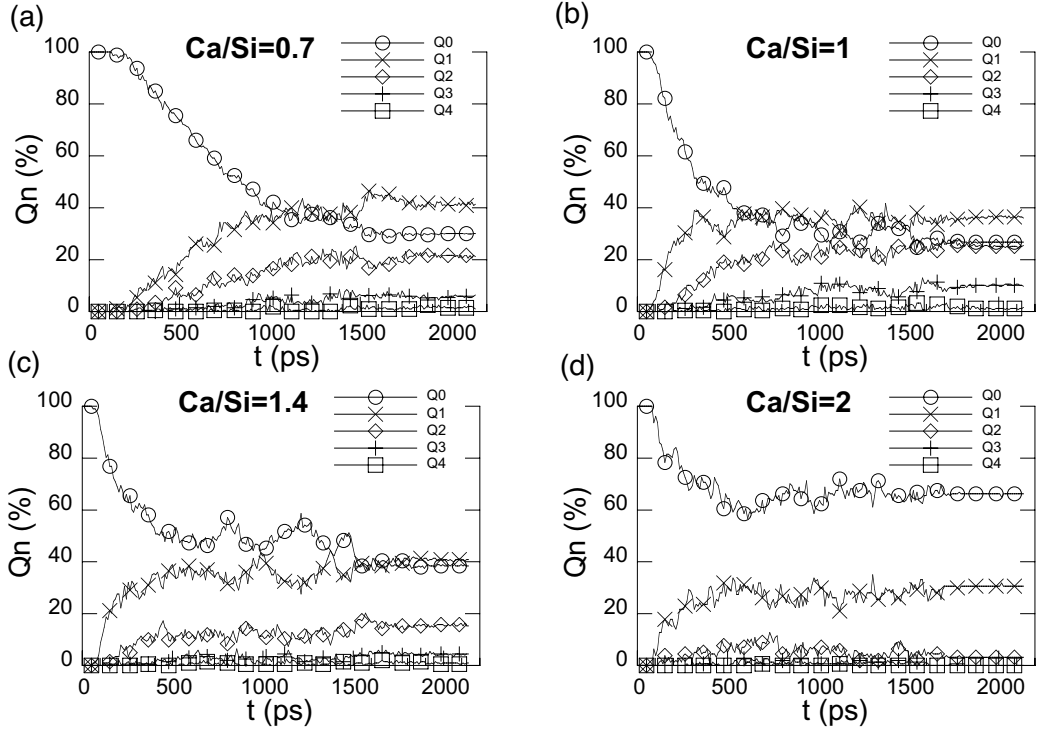


Figure 1: Time evolution of the Q_n peaks for (a) $\text{Ca}/\text{Si}=0.7$, (b) $\text{Ca}/\text{Si}=1$, (c) $\text{Ca}/\text{Si}=1.4$ and (d) $\text{Ca}/\text{Si}=2$.

silicate chains as those found in 1.1-nm tobermorite crystals.

An important parameter to assess the connectivity of the silicate chains of C-S-H gels is the so-called Q factor [35]. This parameter is defined as $Q=Q_1/(Q_1+Q_2+Q_3)$, and represents, up to a factor two, the inverse of the mean chain length. In Figure 2 (b) our calculations (solid points) of the Q factors are represented as a function of the Ca/Si ratio. For comparison we also show the results of the ^{29}Si NMR measurements which were performed by Cong and Kirkpatrick [4] (squares). Additionally we display the Q factors of 1.4-nm tobermorite and jennite (dashed and solid lines respectively). Our results are in reasonable agreement with the experimental values. On the one hand, the trend is reproduced that shorter (higher Q values) chains are formed when the Ca/Si ratio increases. On the other hand, our simulation results for the Q factors turn out to be between the range of tobermorite and jennite structures for Ca/Si ratios between $\text{Ca}/\text{Si} \approx 1$ and $\text{Ca}/\text{Si} \approx 2$. However, there are slight but important differences between our results and the predictions provided in Ref. [4] that should be highlighted. Although for low Ca/Si ratios our simulated Q factors support a close proximity to 1.4-nm tobermorite, at high Ca/Si ratios (above $\text{Ca}/\text{Si} 1.4$) our simulations are clearly biased towards jennite-like structures. In Ref. [4],

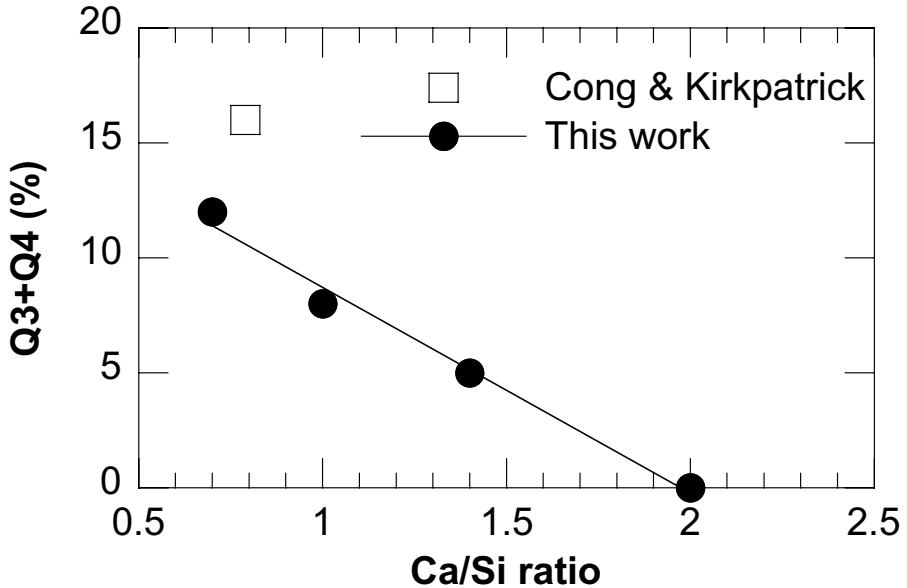
the presence of local jennite-like features was suggested to be due to possible portlandite regions. To explore such a possibility we analyzed the snapshots of our simulations and computed the pair correlation radial distributions [36]. No portlandite morphologies were recognized. Therefore, our results can not be explained in terms of a mixture of tobermorite-like elements and small portlandite regions. On the contrary, in terms of the Q factor our simulations indicate the importance of jennite morphologies in appropriate structural models of C-S-H at high Ca/Si ratios.

3.2 Si-OH and Ca-OH Bonds

A key difference between jennite and 1.4-nm tobermorite is the presence of Si-OH and Ca-OH bonds. In fact, both the Si-OH and Ca-OH bonds are known to be crucial in determining the local nanostructure of C-S-H gels [4, 6, 13]. The results of different IR [10] and ^{29}Si NMR experiments [4] have suggested that the protons of Si-OH bonds are first replaced by interlayer Ca, and only later by Ca-OH groups for raising Ca/Si ratio. In Figure 3 we give the calculated amounts of Si-OH/Si (a) and Ca-OH/Ca bonds (b), respectively, as a function of the Ca/Si ratio. We also show in Figure 3 the estimations given by the charge-balance calculations presented in Ref. [4]. In Figure 3 (b), the data obtained by Thomas et al. [13] by inelastic neutron spectroscopy (INS) over leached pastes are also plotted.

In accordance with the experimentally observed trend, the concentration of Si-OH bonds in the C-S-H gel decreases with an increase of the Ca/Si ratio. Note also that there is an overall good agreement between our simulations and the estimations provided by the charge-balance calculations. This suggests that, in general, the picture given by this simple charge-balance model suffices to qualitatively reproduce the chemistry of the Si-OH groups. However, at high Ca/Si ratios (above 1.5), our simulations do not exhibit a specific decay in the percentage of Si-OH bonds. For Ca/Si=2, our simulations predict $\text{Si-OH/Si} \approx 0.12$ whereas the charge-balance model gives an almost negligible value. Note that for perfect jennite crystals there are no Si-OH bonds, while for 1.4-nm tobermorite crystals the number of Si-OH bonds per Si tetrahedron amounts to 0.333. Thus, in terms of the Si-OH bonds, our simulations produce C-S-H gels with silicate chains that resemble more tobermorite structures than jennite-like arrangements. We conclude that even at high Ca/Si ratios a certain content of tobermorite-like must be present in C-S-H gels.

(a)



(b)

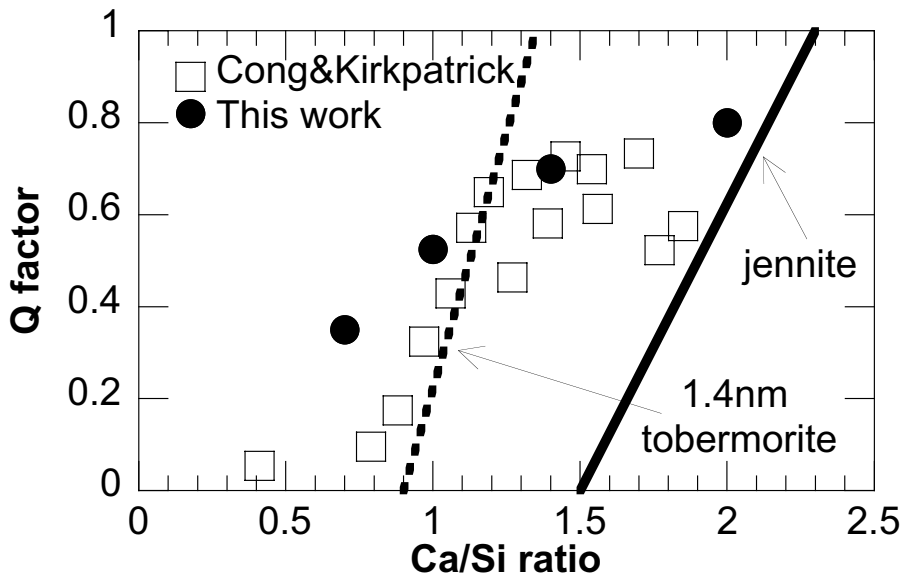
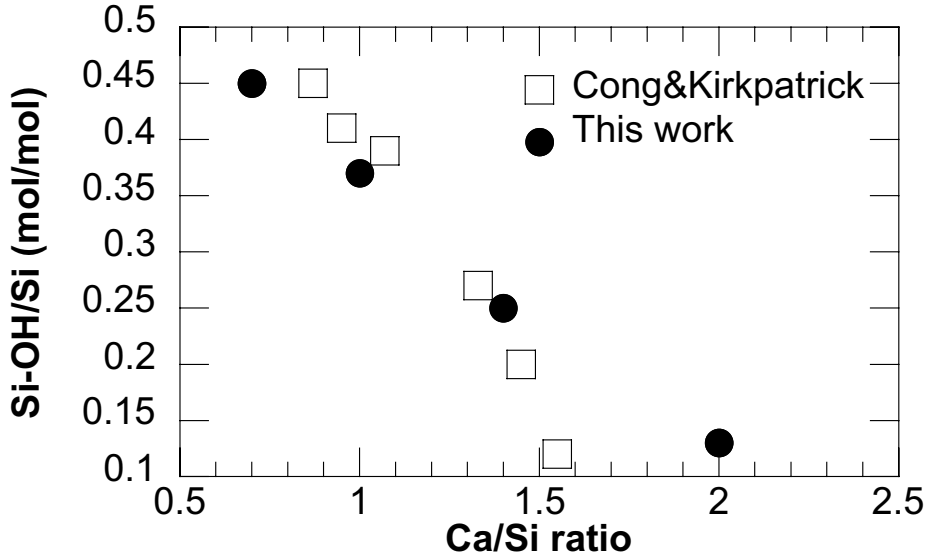


Figure 2: (a) To assess the percentage of non-linear structures, we have computed the sum Q_3+Q_4 as a function of Ca/Si ratio (solid points). The best linear fit is represented by a solid line. (b) Q factor as a function of the Ca/Si ratio. Our simulations (solid points) are compared with the experimental data provided by Cong and Kirkpatrick [4] (squares). The values of perfect 1.4-nm tobermorite (dashed line) and jennite (solid line) are also represented.

(a)



(b)

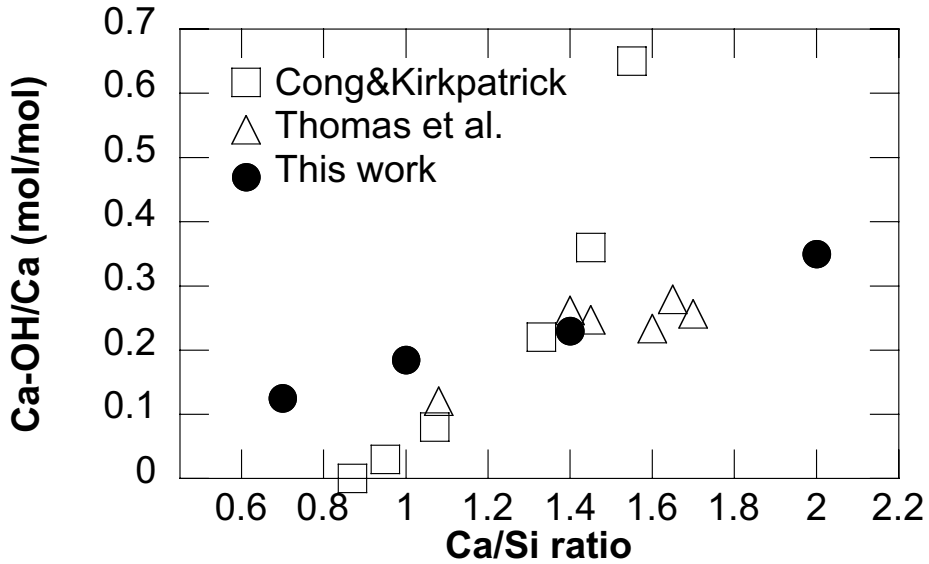


Figure 3: (a) Number of Si-OH/Si bonds as a function of the Ca/Si ratio, as determined by the charge balance model proposed by Cong and Kirkpatrick [4] (squares), and those calculated in this work (solid points). (b) Number of Ca-OH/Ca bonds as a function of the Ca/Si as determined by the charge balance model proposed by Cong and Kirkpatrick [4] (squares), the experimental data of Thomas et al. [13] (triangles), and those calculated in this work (solid points).

Complementary information of the nanostructure of the C-S-H gel can be obtained in terms of the number of Ca-OH bonds, see Figure 3 (b). Although for the Ca/Si ratio in the range 1 to 1.5 there is a reasonable agreement between our calculations and the estimations given by the charge-balance method, very different predictions are obtained below and above this range. In general, our simulations show a moderate increase in the number of Ca-OH bonds with increasing Ca/Si ratios, but do not result in the sudden fall (raise) that the charge-balance model predicts at low (high) Ca/Si ratios. In fact, at high Ca/Si ratios (e.g. above 1.4), we found Ca-OH/Ca values that are still close to 0.3 whereas the values predicted by the charge-balance calculations are well above 0.7. But note that – at these high Ca/Si ratios – our results seem to reasonably agree with the values obtained by Thomas et al. [13] by INS. This suggests that in terms of the Ca-OH local ordination, our simulated C-S-H gels resemble jennite-like structures. For perfect tobermorite-like structures there are no Ca-OH bonds, whereas the value Ca-OH/Ca for jennite crystals is 0.333. Thus, the results of our simulations seem to agree with the conclusions of Ref. [13] that suggest that – for high Ca/Si ratios – the local structure of C-S-H resembles that of jennite. At low Ca/Si ratios (e.g. below Ca/Si=1), we found larger amounts of Ca-OH bonds than expected by the charge-balance estimation. This fact suggests that even at low Ca/Si ratios our simulations reproduce certain jennite-like features.

Hence, our results fit well with the structural models discussed in Ref. [2, 3], which state that cementitious C-S-H gels simultaneously exhibit tobermorite and jennite features. A possible structural explanation of our simulated C-S-H gels is the following: At low Ca/Si ratios, and due to low Q values, long chains are required, probably pentamers and longer chains. Moreover, the presence of Ca-OH bonds suffices to guarantee some jennite-like content. On the other hand, the Si-OH/Si values support the predominant role of 1.4-nm tobermorite-like configurations. The possibility of some 1.1-nm tobermorite content fits well with the appearance of Q3 peaks and the high content of Si-OH bonds. At high Ca/Si ratios, the high Q factors require low polymerized structures, probably dimers. Moreover, the high Ca-OH/Ca values suggest that the predominant structural model must be jennite. However, the presence of Si-OH bonds can only be explained if a certain content of tobermorite remains. In between there is a gradual evolution from long to short chains, and from tobermorite-like to jennite-like features.

4 Summary and Conclusions

In this work we studied the formation of C-S-H structures by means of a molecular dynamics simulation of the polymerization of silicic acids ($\text{Si}(\text{OH})_4$) in presence of solvated calcium ions ($\text{Ca}(\text{OH})_2 \cdot 4\text{H}_2\text{O}$).

Our calculations show that the presence of Ca ions perturbs the polymeriza-

tion of silica sols. In fact we observe that when the Ca/Si ratio is raised, the polymerization degree is clearly reduced. Our simulations also reveal that the polymerization is constrained to linear forms. Only at low Ca/Si ratios certain amounts of Q_{3+Q₄} (%) remain. We also computed the Q factors for different Ca/Si ratios and compared them with the existing experimental data. We basically found a reasonable agreement with experiment. On the one hand, our simulations reproduce the fact that long chains (i.e. low Q factors) are related to low Ca/Si ratios, whereas short chains (high Q factors) are due to low Ca/Si ratios. On the other hand, our computed Q factors lay in the range between tobermorite and jennite crystals for Ca/Si ratios between Ca/Si \approx 1 and Ca/Si \approx 2. We also discussed the appearance of 1.4-nm tobermorite and jennite structures in terms of these Q factors. We came to the conclusion that at low Ca/Si ratios, 1.4-nm tobermorite is an appropriate structural model of C-S-H gels, whereas at high Ca/Si ratios, our simulated C-S-H gels resemble jennite-like arrangements.

Our calculations also provide information about the content of Ca-OH and Si-OH bonds. Here, the simulations reproduce the experimentally observed trend: The number of Ca-OH bonds increase with the Ca/Si ratio whereas the Si-OH bonds decrease. For low Ca/Si ratios, our computed numbers of Si-OH/Si bonds seem to be consistent with the existence of tobermorite configurations. Moreover, the significant amounts of Ca-OH bonds that we have found suggest that certain jennite-like features must be also present. At high Ca/Si ratios, our simulated C-S-H gels reasonably follow the values of Ca-OH/Ca obtained through INS by Thomas et al. [13], which supports their hypothesis that jennite is the best structural model of C-S-H gels. However, the non-negligible amount of Si-OH bonds that we obtain can not be explained without some additional tobermorite-like features.

Finally, we propose a possible structural explanation of our simulated C-S-H gels as follows: At low Ca/Si ratios, our simulated C-S-H systems could be seen as mixtures of long polymerized (pentamers and longer chains) 1.1-nm tobermorite, 1.4-nm tobermorite and jennite structures, whereas at high Ca/Si ratios they seem to be composed of short (dimers) 1.4-nm tobermorite and jennite pieces. In between, there is a gradual evolution from long to short chains, and from tobermorite-like to jennite-like features.

Acknowledgments

We thank L. Jager and R. Wildenhues, who were involved in the development of the molecular dynamics software package TREMOLO of the Institut for Numerical Simulation.

References

- [1] V. S. Ramachandran and J. Beaudoin. *Handbook of Analytical Techniques in Concrete Science and Technology*. Building Materials Series. 2001.
- [2] H. F. Taylor. Proposed structure for calcium silicate hydrate gel. *J. Am. Ceram. Soc.*, 73(6):464–467, 1986.
- [3] I. G. Richardson and G. W. Groves. Models for the composition and structure of calcium silicate hydrate (C-S-H) gel in hardened tricalcium silicate pastes. *Cement and Concrete Research*, 22:1001–1010, 1992.
- [4] X. Cong and R. J. Kirkpatrick. ^{29}Si MAS NMR study of the structure of calcium silicate hydrate. *Adv. Cem. Based Mater.*, 3:144–146, 1996.
- [5] A. Nonat and X. Lecoq. The structure, stoichiometry and properties of C-S-H prepared by C_3S hydration under controlled conditions. In P. Colombet, A. R. Grimmer, H. Zanni, and P. Sozzani, editors, *Nuclear Magnetic Resonance Spectroscopy of Cement-Based Materials*, pages 197–207. Springer, Berlin, 1998.
- [6] J. J. Chen, J. T. Thomas, H. F. Taylor, and H. M. Jennings. Solubility and structure of calcium silicate hydrate. *Cement and Concrete Research*, 34: 1499–1519, 2004.
- [7] I. G. Richardson. obermorite/jennite and tobermorite/calcium hydroxide-based models for the structure of C-S-H: Applicability to hardened pastes of tricalcium silicate, b-dicalcium silicate, Portland cement, and blends of Portland cement with blast-furnace, metakaolin, or silica fume. *Cement and Concrete Research*, 34:1733–1777, 2004.
- [8] A. R. Brough, C. M. Dobson, I. G. Richardson, and G. W. Groves. In situ solid state NMR studies of Ca_3SiO_5 : Hydration at room temperature and at elevated temperatures using ^{29}Si enrichment. *Journal of Materials Science*, 29:3926–3940, 1994.
- [9] X. Cong and R. J. Kirkpatrick. ^{17}O MAS NMR investigation of the structure of the calcium silicate hydrate gel. *J. Am. Ceram. Soc.*, 79(6):1585–1592, 1996.
- [10] P. Yu, R. J. Kirkpatrick, B. Poe, P. F. McMillan, and X. Cong. Structure of calcium silicate hydrate (C-S-H): Near-, mid-, and far-infrared spectroscopy. *J. Am. Ceram. Soc.*, 82(3):742–748, 1999.
- [11] D. Viehland, L. J. Yuan, Z. Xu, X. Cong, and R. J. Kirkpatrick. Structural studies of jennite and 1.4 nm tobermorite: Distorted layering along the [100] of jennite. *J. Am. Ceram. Soc.*, 80(12):3021–3028, 1997.

- [12] X. Zhang, W. Chang, T. Zhang, and C. K. Ong. Nanostructure of calcium silicate hydrate gels in cement paste. *J. Am. Ceram. Soc.*, 83(10):2600–2604, 2000.
- [13] J. J. Thomas, J. Chen, H. M. Jennings, and D. A. Neumann. Ca-OH bonding in the C-S-H gel of tricalcium silicate and white Portland cement pastes measured by inelastic neutron scattering. *Chem. Mater.*, 15(20):3813–3817, 2003.
- [14] B. Jönsson, A. Nonat, C. Labbez, B. Cabane, and H. Wennerström. Controlling the cohesion of cement paste. *Langmuir*, 21(20):9211–9221, 2005.
- [15] B. Derjaguin and L. D. Landau. Theory of the stability of strongly charged lyophobic sols and of the adhesion of strongly charged particles in solution of electrolytes. *Acta Physicochim URSS*, 14:635–662, 1941.
- [16] E. W. J. Verwey and J. Th. G. Overbeek. *Theory of the stability of lyophobic colloids*. Elsevier, New York, 1948.
- [17] R. J.-M. Pellenq, J. M. Caillol, and A. Delville. Electrostatic attraction between two charged surfaces: A (N,V,T) Monte Carlo simulation. *J. Phys. Chem. B*, 101(42):8584–8594, 1997.
- [18] A. Delville and R. J.-M. Pellenq. Electrostatic attraction and/or repulsion between charged colloids: A (NVT) Monte-Carlo study. *Molecular Simulation*, 24:1–24, 2000.
- [19] A. Gmira, M. Zabat, R. J.-M. Pellenq, and H. Van Damme. Microscopic physical basis of the poromechanical behavior of cement-based materials. *Materials and Structures/Concrete Science and Engineering*, 37:3–14, 2004.
- [20] P. Faucon, J. M. Delaye, J. Virlet, J. F. Jacquinot, and F. Adenot. Study of the structural properties of the C-S-H(I) by molecular dynamics simulations. *Cem. Concr. Res.*, 27:1581–1590, 1997.
- [21] A. Kalinitchev, J. Wang, and R. J. Kirkpatrick. Molecular dynamics modeling of the structure, dynamics and energetics of mineral-water interfaces: Applications to cement materials. *Cem. Concr. Res.*, 37:337–347, 2007.
- [22] H. Manzano, A. Ayuela, and J. S. Dolado. On the formation of cementitious C-S-H nanoparticles. *Journal of Computer-Aided Materials Design*, 14(1): 45–51, 2007.
- [23] B. P. Feuston and S. H. Garofallini. Onset of polymerisation in silica sols. *Chem. Phys. Lett.*, 170:264–270, 1990.

- [24] F. Stillinger and T. Weber. Computer simulation of local order in condensed phases of silicon. *Phys. Rev. B*, 31:5262–5271, 1985.
- [25] D. A. Litton and S. H. Garofalini. Modeling of hydrophilic wafer bonding by molecular dynamics simulations. *J. Appl. Phys.*, 89(11):6013–6023, 2001.
- [26] X. Su and S. H. Garofalini. Role of nitrogen on the atomistic structure of the intergranular film in silicon nitride: A molecular dynamics study. *J. Mater. Res.*, 19:3679–3678, 2004.
- [27] S. Nosé and M. L. Klein. Constant pressure molecular dynamics for molecular systems. *Molec. Phys.*, 50(5):1055–1076, 1983.
- [28] D. Beeman. Some multistep methods for use in molecular dynamics calculations. *J. Comp. Phys.*, 20:130–139, 1976.
- [29] K. Refson. Molecular dynamics simulation of solid n-butane. *Physica B*, 131:156–266, 1985.
- [30] M. Griebel, S. Knappe, and G. Zumbusch. *Numerical simulation in molecular dynamics; Numerics, algorithms, parallelization, applications*, volume 5 of *Texts in Computational Science and Engineering*. Springer, Heidelberg, 2007.
- [31] Himalaya is the high-performance cluster computer of the Institute for Numerical Simulation and the Sonderforschungsbereich 611 at the University of Bonn. Himalaya achieves 1269 GFlop/s in the Linpack benchmark test and was ranked number 428 on the June 2005 Top500 list. See also the web page. See also the web page <http://wissrech.ins.uni-bonn.de/research/himalaya/index.html>.
- [32] M. Griebel and J. Hamaekers. Molecular dynamics simulations of the mechanical properties of polyethylene-carbon nanotube composites. In M. Rieth and W. Schommers, editors, *Handbook of Theoretical and Computational Nanotechnology*, volume 9, chapter 8, pages 409–454. American Scientific Publishers, 2006.
- [33] S. H. Garofalini and G. E. Martin. Molecular simulations of the polymerization of silicic acid molecules and network. *J. Phys. Chem.*, 98(4):1311–1316, 1994.
- [34] J. Bensted and P. Barnes, editors. *Structure and performance of cements*. Spon Press, London, second edition, 2002.
- [35] J. J. Thomas and H. M. Jennings. Free-energy-based model of chemical equilibria in the CaO-SiO₂-H₂O system. *J. Am. Ceram. Soc.*, 81(31):606–612, 1998.

- [36] J. S. Dolado, M. Griebel, and J. Hamaekers. The role of calcium ions in the polymerization of silicic acids: A molecular dynamic study. In preparation.